Biogeochemistry **44:** 29–49, 1999.

Estimation of annual nitrous oxide emissions from a transitional grassland-forest region in Saskatchewan, Canada

MARIFE D. CORRE[1,2,*], DANIEL J. PENNOCK[1], CHRIS VAN KESSEL[1,3] & D. KIRK ELLIOTT[1]
[1]*Department of Soil Science, University of Saskatchewan, Saskatoon, Saskatchewan S7N 5A8, Canada;* [2]*Present address: Pasture Systems and Watershed Management Research, USDA-ARS, Curtin Road, University Park, PA 16802, USA;* [3]*Present address: Department of Agronomy and Range Science, University of California, Davis, CA 95616 USA*
*(*Corresponding author: E-mail: mdc7@psu.edu. Contribution no. R824 of Saskatchewan Center for Soil Research, Saskatoon, Saskatchewan, Canada)*

Accepted 30 March 1998

Key words: GIS database, landscape scale, nitrous oxide, regional scale

Abstract. The increasing atmospheric N_2O concentration and the imbalance in its global budget have triggered the interest in quantifying N_2O fluxes from various ecosystems. This study was conducted to estimate the annual N_2O emissions from a transitional grassland-forest region in Saskatchewan, Canada. The study region was stratified according to soil texture and land use types, and we selected seven landscapes (sites) to cover the range of soil texture and land use characteristics in the region. The study sites were, in turn, stratified into distinguishable spatial sampling units (i.e., footslope and shoulder complexes), which reflected the differences in soils and soil moisture regimes within a landscape. N_2O emission was measured using a sealed chamber method. Our results showed that water-filled pore space (WFPS) was the variable most correlated to N_2O fluxes. With this finding, we estimated the total N_2O emissions by using regression equations that relate WFPS to N_2O emission, and linking these regression equations with a soil moisture model for predicting WFPS. The average annual fluxes from fertilized cropland, pasture/hay land, and forest areas were 2.00, 0.04, and 0.02 kg N_2O-N ha^{-1} yr^{-1}, respectively. The average annual fluxes for the medium- to fine-textured and sandy-textured areas were 1.40 and 0.04 kg N_2O-N ha^{-1} yr^{-1}, respectively. The weighted-average annual flux for the study region is 0.95 kg N_2O-N ha^{-1} yr^{-1}. The fertilized cropped areas covered only 47% of the regional area but contributed about 98% of the regional flux. We found that in the clay loam, cropped site, 2% and 3% of the applied fertilizer were emitted as N_2O on the shoulders and footslopes, respectively.

Introduction

N_2O contributes 5% of the global warming potential in the assessment of the greenhouse effect (Rodhe 1990). It has also been implicated as the major natural regulator of the stratospheric O_3 (Crutzen & Ehhalt 1977), which controls the earth's ultraviolet-B radiation balance. The atmospheric N_2O concentration has been rising over the last twenty years at the rate of 0.25% yr^{-1} (Khalil & Rasmussen 1992), and its global budget seems to be not in balance (estimates of global sources are 30% lower than estimates of global sinks; Watson et al. 1990; Robertson 1993). The imbalance in its global budget could be due to the lack of information on fluxes from other important ecosystems. For example, in areas of semiarid to subhumid cold continental climate (i.e., Prairie Provinces of Canada – Alberta, Saskatchewan, and Manitoba), data on N_2O emissions are scanty. From these areas, N_2O emissions from undisturbed natural ecosystems are also not known. In Saskatchewan, earlier studies on N losses from agricultural soils mainly focused on denitrification. Denitrification is only one of the processes contributing to N_2O production in the soil, and denitrification losses cannot just simply be related to N_2O evolution (Weier et al. 1993).

The major difficulty in quantifying annual N_2O fluxes at the landscape and regional scales is the high degree of spatial and temporal variability of N_2O emission. Many recent review papers (e.g., Schimel et al. 1988; Matson et al. 1989; Groffman 1991; Robertson 1993; Schimel & Potter 1995) have addressed investigation strategies for dealing with the characteristically high variability of N_2O emission. Improved assessment of N_2O emission requires techniques for reducing random variation within experimental units (e.g., landscape), and knowledge of the factors that result in systematic variation among landscapes and across seasons. To address these investigation strategies, we measured N_2O emission from 1993 to 1995 in seven sites selected to cover the range of soil texture and land use characteristics in a transitional grassland-forest region of the Black soil zone (Udic Boroll) in Saskatchewan, Canada. The selection of the study sites in the delineated study region (about 63 km by 74 km) was governed by the present understanding of the regional controls on N_2O emission. Both field-based research (Groffman & Tiedje 1989; Mosier et al. 1996) and existing models of N_2O emission (Li et al. 1992; Parton et al. 1996; Potter et al. 1996) suggest that soil texture and land use exert a strong, indirect control on N_2O emissions at the regional scale. Soil texture was the proxy variable used to represent the differences in soil moisture regimes and soil fertility, whereas land use was the surrogate variable used to reflect the differences in N and C availability.

Our study region was stratified into three main textural areas: moderately fine to fine (primarily glacio-lacustrine clay to clay loam parent sediments), medium (primarily glacio-lacustrine silts to very fine sands), and sandy areas (primarily glacio-fluvial sands; Acton & Ellis 1978). Clay loam, fine sandy loam, and sandy study areas were chosen to represent the aforementioned three textural areas, respectively. In the clay loam area, a long-term (broken prior to 1920) cropped site, a pasture, and a forest site were selected. In the fine sandy loam area, a long-term cropped site was chosen, and in the sandy area, a cropped site, a pasture, and a forest site were selected.

The study sites were, in turn, stratified into two spatial sampling units (i.e., shoulder and footslope complexes) from which measurement of N_2O fluxes and comparison of activity among sites were based. These two sampling units represented the two major soil-landform assemblages in the study sites: the shoulder complex of which Orthic Regosols (Typic Udorthent) and Orthic Black Chernozems (Udic Haploboroll) dominate, and the footslope complex of which aside from Orthic Black Chernozems, Gleyed Black Chernozems (Udic Haploboroll) and Gleysols (Typic Haplaquoll) also occurred (Corre 1997). These soil-slope associations reflect the action and interaction of hydrological and geomorphic processes, which showed a progression from the dry to the wet soils on the shoulder to the footslope complexes (Pennock et al. 1987).

From this transitional grassland-forest region, the landscape and seasonal patterns of N_2O oxide emission and the factors controlling such patterns were reported earlier (Corre et al. 1996). The data (N_2O fluxes measured at discrete sampling days) from Corre et al. (1996) were used in the present study to estimate the annual N_2O emissions at the landscape and regional scales using simple integrative method for seasonal interpolation of fluxes and geographic information systems for spatial extrapolation of fluxes.

Materials and methods

Site description, and measurement of N_2O fluxes, soil and climatic variables

In the clay loam area, the cropped site was seeded to unfertilized canola (*Brassica rapa* L.) in 1993 and to fertilized wheat (*Triticum aestivum* L.) in 1994 (fertilized with 28 kg N ha^{-1} (anhydrous NH_3) at seeding (May 11) and 57 kg N ha^{-1} (urea) at seedling stage (June 10)). The clay loam, pasture and forest sites were situated adjacent to each other. The pasture site (converted from forest 20 years previously) was located on the shoulder portion of the landscape and was dominated mainly by smooth bromegrass (*Bromus inermis* Leysser). The forest site was located on the footslope portion of the landscape and was occupied by aspen (*Populus tremuloides* Michaux). The N_2O emissions from these three sites were measured from May 1993 to May 1995. In the fine sandy loam area, the cropped site was planted to canola and was fertilized with 62 kg N ha^{-1} (anhydrous NH_3) at seeding (15 June 1994). The N_2O emissions from this site were measured from May 1994 to May

1995. In the sandy area, the cropped site was planted to oat (*Avena sativa* L.) and was fertilized with 45 kg N ha^{-1} (ammonium sulfate) at seeding (10 June 1994). The sandy, pasture site was seeded to alfalfa (*Medicago sativa* L.), and the sandy, forest site has continuous aspen cover. The N_2O emissions from these three sites were measured from June 1994 to May 1995.

During summer, N_2O emissions were measured thrice a month. In fall, measurements were taken once a month until the activity was undetectable (when the soil was frozen (October) and later on covered with snow (early November)). Measurements were resumed at weekly interval during the spring thaw. On any given sampling day, N_2O emissions were measured from all sites at the same time of the day (between 10:00 a.m. to 2:00 p.m.).

Direct in-field measurement of N_2O emission was carried out using a sealed chamber method. At each shoulder and footslope complexes, at least ten sampling points were selected randomly from a grid sampling design with 15-m spacing, so that any sampling points that happened to be selected adjacent to each other had a distance of 15 m. The description of the sealed chamber, gas sampling method, N_2O concentration analysis, and calculation of vertical flux density were reported earlier (Corre et al. 1996). The water-filled pore space (WFPS; ratio of the volumetric moisture content to the total pore space) was measured in all N_2O sampling days, except when the soil was covered with snow. Soil mineral N (NH_4^+, and NO_2^- + NO_3^-) and soluble organic C were measured once a month and were determined following the procedures described in Pennock et al. (1992). Other soil characteristics (Table 1) were also measured at the start of the study. All soil variables were measured at 0 to 15-cm depth. Precipitation and air temperature (at 1.5 m above the ground) were recorded continuously by an on-site meteorological station located in the center of the study region. The region has mean January and July air temperatures of −20 °C and 16 °C, respectively. The total rainfall was 388 mm in 1993 and 401 mm in 1994. The total snowfall was 90 mm from fall 1993 to spring 1994 and 147 mm from fall 1994 to spring 1995. Based on the 50-yr climatic record of this study region, the total precipitation and air temperatures in 1993 to 1995 were in the normal range.

Temporal interpolation of fluxes from summer to fall and in spring

As shown in our earlier study (Corre et al. 1996), we observed similar seasonal patterns of N_2O emissions and soil moisture, which were related to the rainfall distribution pattern during the summer and to the melting of snow and thawing of soil during the spring. The N_2O emission increased towards early summer (about 70% of the total annual rainfall occurred from late May to mid-July), decreased towards late summer (only low levels of rainfall occurred intermittently from late July to September), and ceased by

Table 1. Soil characteristics measured at 0 to 15-cm depth.

Study sites	Land use	Landform complex	Sand	Silt	Clay	Saturation moisture content	Field capacity	Permanent wilting point	Total N	Total C
				(%)			(%; v/v)		($Mg\ ha^{-1}$)	
Clay loam	Cropped	Shoulder	31	37	32	50	39	22	5.0	59.8
		Footslope	31	38	31	56	40	21	6.5	79.2
	Pasture	Shoulder	26	42	32	55	41	25	6.2	78.7
	Forest	Footslope	22	48	30	67	41	28	7.2	94.0
Fine sandy loam	Cropped	Shoulder	52	27	21	49	30	18	4.1	47.6
		Footslope	48	29	23	54	31	19	6.5	64.5
Sandy	Cropped	Shoulder	88	6	6	50	13	7	1.6	27.6
		Footslope	85	8	7	54	14	7	2.4	28.8
	Pasture	Shoulder	87	8	5	44	13	7	6.2	51.2
		Footslope	82	12	6	63	16	9	5.1	39.6
	Forest	Shoulder	87	7	6	60	15	9	2.7	40.6
		Footslope	85	9	6	58	16	9	2.5	40.5

the onset of frost in fall. The presence of frozen soil layer and snow cover during fall to winter had prevented gas efflux during this period. N_2O emission activity was only again detected in spring (the start of spring thaw generally occurred in mid-March; Corre et al. 1996). This seasonal fluctuation of N_2O emission illustrates that a simple interpolation between discrete sampling days would not give a good estimate of total N_2O emission during summer to fall (i.e., May to October). One reliable method of temporally interpolating fluxes could be that of relating N_2O emissions with WFPS (i.e., regression equations) and linking these regression equations with a soil moisture model for predicting WFPS. A simple soil moisture model, Versatile Soil Moisture Budget (VSMB), that has been tested to work in Saskatchewan (Elliott & de Jong 1992) was used. Estimates of N_2O emissions from May to October were obtained by summing the predicted daily N_2O fluxes from the regression equations, in which the WFPS values were simulated using the VSMB. For a particular study site, the simulation of WFPS by VSMB was done during the year in which the N_2O emissions were measured.

The VSMB was adapted from the modified version of Elliott & de Jong (1992). The driving soil variables for VSMB are soil texture, saturation moisture content, field capacity, and permanent wilting point (Table 1), while the driving climatic variables are daily rainfall, and daily maximum and minimum air temperatures (taken from the climatic station located at the center of the study region). The maximum and minimum daily air temperatures were used to predict latent evaporation following method I of Baier & Robertson (1965). Latent evaporation was converted to potential evapotranspiration using a crop factor which depended on the nature of the crop and its growth stage (Krogman & Hobbs 1976). Evapotranspiration extracted water until the permanent wilting point was reached. Texture and land use were used as the basis for partitioning the rainfall into infiltration and runoff, referring to the Soil Conservation Service Method discussed by Schwab et al. (1993). Following rain, soil moisture was allowed to increase to the saturation moisture content and drainage occurred when the soil was between saturation and field capacity. For the clay loam and fine sandy loam sites, it was assumed that 75% of the moisture excess of the field capacity drained in 24 h and that field capacity was reached in 2 d. For the sandy sites, it was assumed that 100% of the moisture excess of the field capacity drained in 24 h. At the end of each day, the gains and losses of water were summed and new moisture contents were calculated.

The total N_2O emission in spring (i.e., mid-March to April) was estimated using simple interpolation of fluxes (i.e., trapezoidal quadrature calculation) measured at discrete sampling days. It is not possible to predict N_2O emissions from WFPS during the spring using only a simplified soil moisture model (i.e., VSMB) that does not deal with the detailed soil water dynamics (e.g., fractions of snow melting, depth of soil thawing, snow redistribution, etc.) during the spring thaw period. The trapezoidal quadrature calculation, however, is considered appropriate for estimating the total N_2O emission in spring because the N_2O flux measurements were taken often enough that they clearly showed the beginning, peak, and end of the spring activity (Corre et al. 1996).

Spatial extrapolation of annual N_2O emissions from landscape to regional scale

The 'measure and multiply' method was used in scaling-up annual N_2O fluxes from landscape to regional scale, as described by Schimel & Potter (1995). This method was employed using geographic information system (GIS) technology where the maps of the ecological variables proven to control N_2O emissions (i.e., land use (Figure 1) and soil texture (Figure 2)) were overlaid to form discrete spatial classes or cells. The land use types in the study region were characterized from a LANDSAT 5 thematic mapper image, containing bands 3 (red, 0.63–0.69 μm), 4 (near infrared, 0.76–0.90 μm) and 5 (middle infrared, 1.55–1.75 μm). This image of the study region was acquired on a cloud-free day (9 August 1991). The Earth Resources Data Analysis Systems (ERDAS Inc., Atlanta, GA) software was used in the image processing and classification. The image was classified using a combination of supervised and unsupervised classification methods. The accuracy of the classification was evaluated by using one hundred ground points of known land use type (different from those used in the classification), and a classification accuracy of 85% was obtained. The data on soil texture were obtained from various sources: ARC/INFO and PAMAP GIS products, and from soil survey maps (encoded into GIS framework using a graphic digitizer). These information were combined into one GIS format using the Spatial Analysis Systems (SPANS; INTERA TYDAC Tech. Inc., Ottawa, Canada). Finally, the land use information was integrated into SPANS, and a matrix of soil texture and land use types was created. The aerial coverage of each class was determined, and these spatial classes were filled with their corresponding annual N_2O fluxes. The measure and multiply method is expressed in equation form as:

$$F = \Sigma\ [A_i F_i]$$

where F is the total flux, A_i is the area of the spatial class i (i.e., specific soil texture and land use characteristics), and F_i is the annual flux from spatial class i. Critical to this approach is the assumption that the N_2O fluxes of the investigated sites are the typical N_2O emission activities of the soil texture and land use categories throughout the study region.

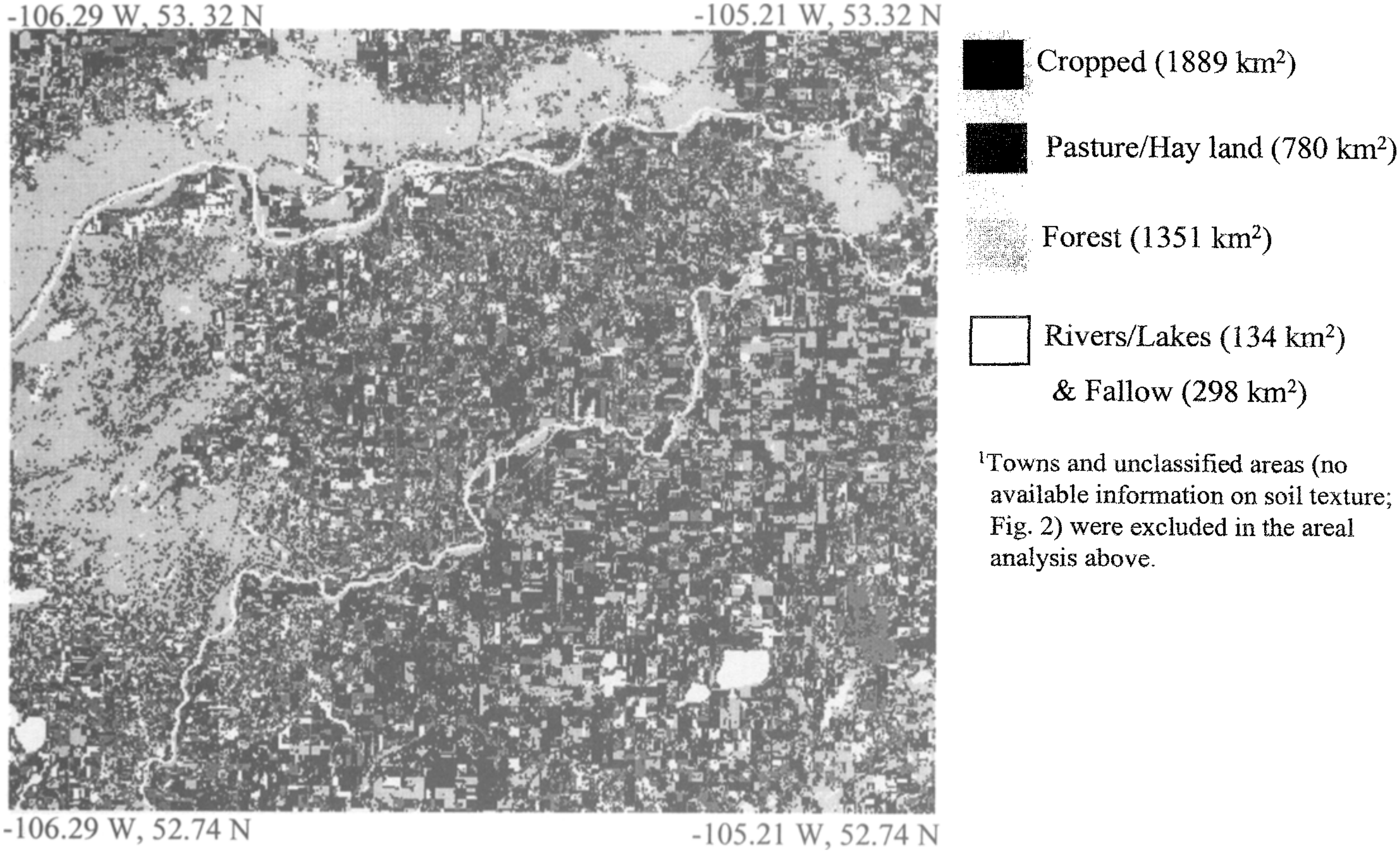

Figure 1. Land use pattern in the study region determined from LANDSAT 5 thematic mapper image.

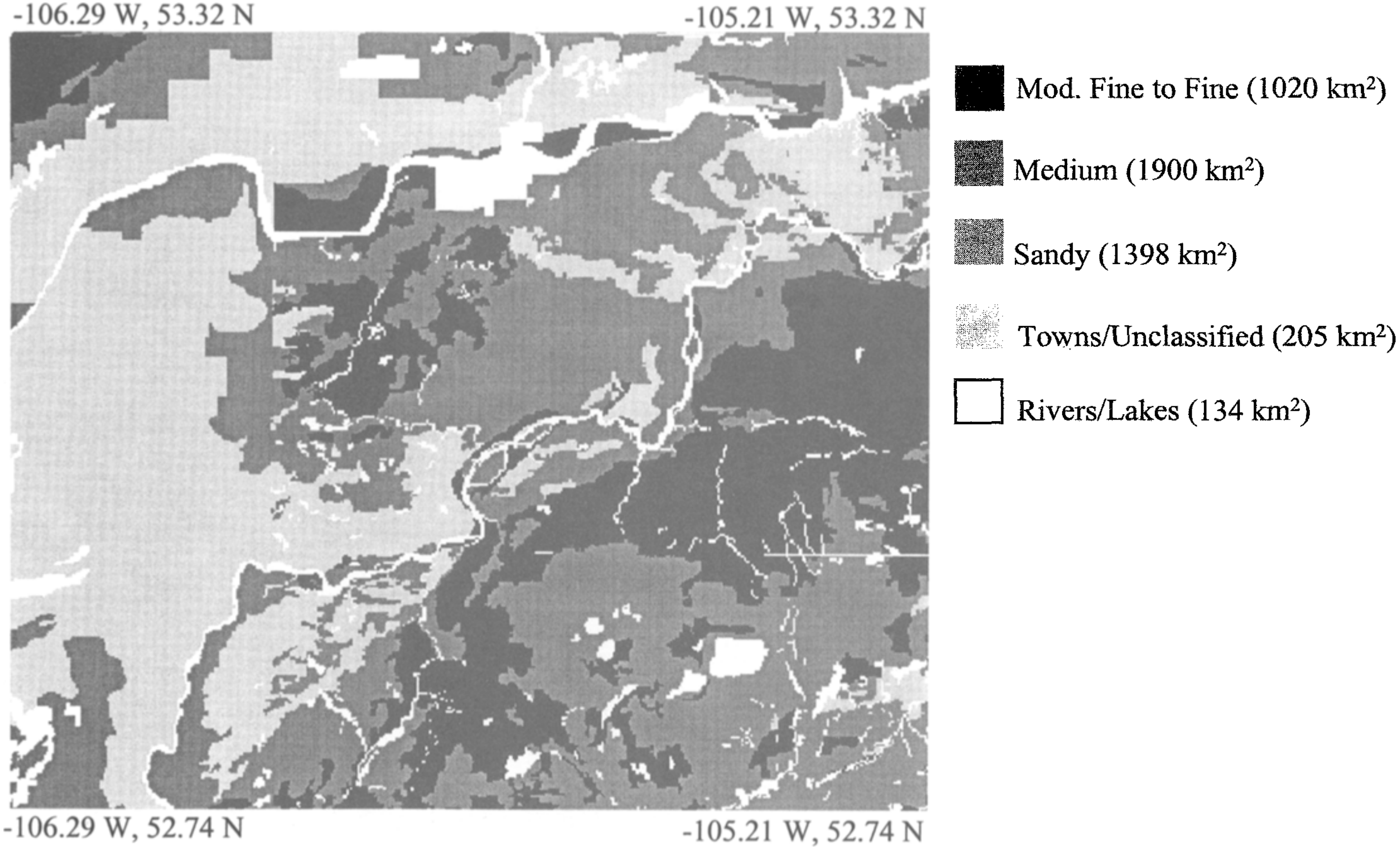

Figure 2. Soil texture characteristics of the study region.

Statistical analyses

The correlation analysis between N_2O fluxes and measured WFPS, NH_4^+, $NO_2^- + NO_3^-$, soluble organic C, rainfall, and maximum air temperature had used the central tendency values of the soil variables on each sampling day (i.e., median of at least ten sampling points on each landform complex at each site), and was conducted considering all the sampling days when both the N_2O emission and the corresponding variable were measured. The regression equations between N_2O fluxes and WFPS were also obtained by considering the median values and was conducted for the data gathered within May to October, as these regression equations were intended to integrate N_2O fluxes also within May to October. The use of the median values could result to a conservative nature of our estimates; however, this conservative statistical measure was preferred in dealing the non-normal nature of N_2O flux data with limited sample numbers.

Results and discussion

Relationships between N_2O emissions and soil and climatic factors

The measured WFPS was the factor most strongly correlated to N_2O emission (Table 2). Related to this factor is the rainfall, which correlated to N_2O emissions in the unfertilized cropped, pasture, and forest sites. In the fertilized cropped sites, rainfall did not show significant correlations because of the confounding effect of fertilization. For example, a particular rainfall level occurring immediately after fertilization showed much higher N_2O fluxes than with the same rainfall level occurring farther from the time of fertilization. There was no clear relationships of N_2O emissions with soil mineral N and soluble C. Others (Schimel et al. 1989; Matson & Vitousek 1990; Davidson & Hackler 1994; Mosier et al. 1996) have also shown that it is difficult to directly correlate *in situ* N_2O fluxes to soil mineral N contents, and that N_2O emissions are related more to the soil N turnover rate rather than mineral N pool size. The lack of significant correlations between N_2O emission and temperature has also been observed in other studies (Myrold 1988; Parsons et al. 1991), and in the present study was a probable consequence of the high N_2O fluxes even at below-zero temperatures in spring.

Predictive relationships for interpolating N_2O fluxes from summer to fall

Separate regression equations (relating N_2O emissions to WFPS) were obtained for different land use types to reflect their differences in N and

Table 2. Pearson correlation coefficients between N_2O emissions and soil and environmental factors. Enclosed in parentheses are the number of sampling days that both N_2O emission and the corresponding variable were measured.

Site	Land form complexes	N_2O vs. Measured WFPS	NH_4^+	NO_3^- + NO_2^-	Soluble organic C	Rainfall	Max. air temperature
Clay loam							
Unfertilized	Shoulder	0.79** (16)	−0.14 ns (5)	−0.93* (5)	(.) (3)	0.62* (19)	0.00 ns (19)
Canola	Footslope	0.71** (16)	−0.43 ns (5)	−0.67 ns (5)	(.) (3)	0.55* (19)	−0.23 ns (19)
Pasture	Shoulder	0.44‡ (19)	−0.35 ns (8)	−0.01 ns (8)	−0.14 ns (8)	0.56** (36)	0.09 ns (36)
Forest	Footslope	0.59* (27)	0.64‡ (8)	0.73† (8)	0.40 ns (8)	0.56** (36)	0.62** (36)
Fertilized	Shoulder	0.49* (18)	0.49 ns (5)	−0.64 ns (5)	−0.23 ns (5)	0.42† (23)	0.02 ns (23)
Wheat	Footslope	0.50† (18)	−0.19 ns (5)	−0.78 ns (5)	−0.08 ns (5)	0.28 ns (23)	0.18 ns (23)
Fine sandy loam							
Fertilized	Shoulder	0.71*** (18)	0.65 ns (5)	−0.26 ns (5)	−0.66 ns (5)	0.36 ns (23)	0.21 ns (23)
Canola	Footslope	0.56* (18)	0.29 ns (5)	0.21 ns (5)	−0.63 ns (5)	0.10 ns (23)	0.12 ns (23)
Sandy							
Fertilized	Shoulder	0.40‡ (14)	0.04 ns (5)	0.57 ns (5)	−0.65 ns (5)	0.40 ns (19)	−0.20 ns (23)
Oat	Footslope	0.50† (14)	−0.44 ns (5)	0.68 ns (5)	−0.25 ns (5)	0.16 ns (19)	−0.23 ns (23)
Pasture	Whole site	0.33‡ (14)	0.58 ns (5)	0.89‡ (5)	−0.10 ns (5)	0.39* (19)	−0.17 ns (23)
Forest	Whole site	0.02 ns (14)	−0.19 ns (5)	(.) (5)	−0.31 ns (5)	0.40† (19)	0.16 ns (23)

*, **, ***, †, ‡ – significant at $\alpha = 0.05$, 0.01, 0.001, 0.10, and 0.20, respectively;
ns – not significant; (.) coefficient cannot be determined.

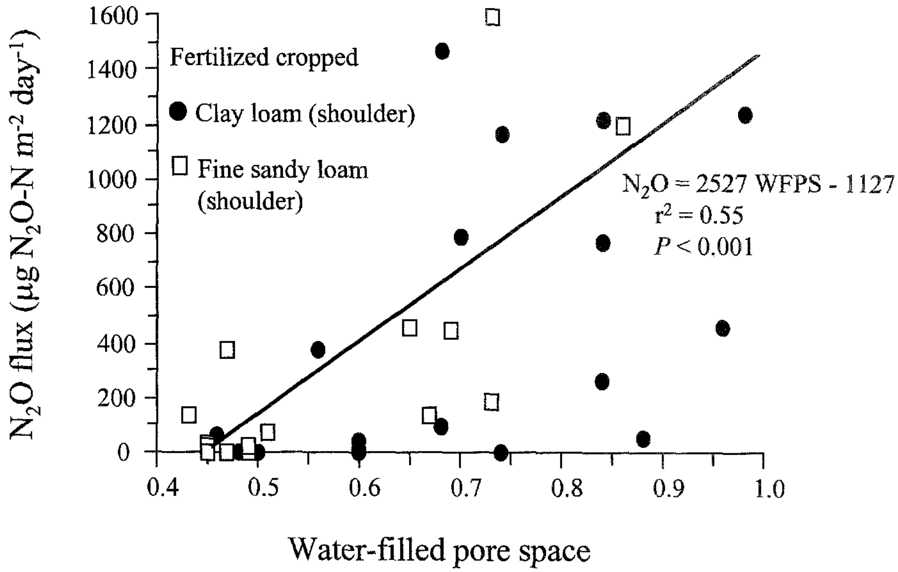

Figure 3. Relationship between field-measured N_2O emissions and water-filled pore space in the clay loam, fertilized wheat and fine sandy loam, fertilized canola sites on the shoulder complex. Each point is a median value of at least ten sampling points.

C availability and thereby eliminating the need for substrate parameters in the regression equations. For a particular land use type, separate regression equations were obtained for different soil textures and landform complexes if the N_2O fluxes from these sampling units have differed (Table 3; graphical example in Figure 3). If otherwise, a land use type was represented only by a single regression equation. The VSMB (for simulating the WFPS), however, was always run separately for each soil texture and landform complex, considering its respective soil characteristics (i.e., texture, saturation moisture content, field capacity, and permanent wilting point; Table 1) that drive the VSMB. The r^2 values of the regressions between N_2O emission and WFPS, although low, are considered respectable, in reference to what others have obtained from field-based studies of N_2O emission. Mosier et al. (1996) obtained r^2 values of 0.23 and 0.29 between N_2O fluxes and WFPS (measured from May to October in semiarid Colorado) from fertilized and unfertilized pastures, respectively.

For the pasture and forest sites, the N_2O emissions were comparable between sites (i.e., between sandy and clay loam sites) and within sites (i.e., between landform complexes in the sandy sites). Hence, the pasture and forest sites were represented each with regression equations that combine the N_2O flux data of both textural sites. There was a good correlation between the

Table 3. Regression equations between N_2O fluxes and water-filed pore space (WFPS) that were used in interpolating N_2O fluxes (μg N_2O-N m^{-2} day^{-1}) from summer to fall. The WFPS was predicted using the Versatile Soil Moisture Budget.

Land use	Regression equations	Coefficient of determination, r^2
Pasture (clay loam and sandy sites)	$N_2O = 27$ WFPS $- 7$	0.23**
Forest (clay loam and sandy sites)	$N_2O = 30$ WFPS $- 9$	0.35***
Unfertilized cropped (clay loam site)		
Shoulder	$N_2O = 139$ WFPS $- 63$	0.45***
Footslope	$N_2O = 745$ WFPS $- 388$	0.51***
Fertilized cropped		
Sandy	$N_2O = 82$ WFPS $- 6$	0.20*
Clay loam & fine sandy loam		
Shoulder	$N_2O = 2527$ WFPS $- 1127$	0.55***
Footslope	$N_2O = 7454$ WFPS $- 3414$	0.24**

measured and predicted WFPS from these sites, ranging from 0.62 ($P = 0.05$) in the sandy, pasture site to 0.81 ($P = 0.001$) in the clay loam, forest site.

For the unfertilized cropped (canola) site in the clay loam area, separate regression equations were obtained for the shoulder and footslope complexes because the N_2O emissions between these landform complexes differed. A similar pattern on measured WFPS was also observed. The measured and predicted WFPS showed correlation coefficients of 0.67 ($P = 0.01$) on the shoulder and 0.57 ($P = 0.05$) on the footslope.

For the fertilized cropped (oat) site in the sandy area, the N_2O emissions between the landform complexes were not different. A similar result was observed with the measured WFPS in all the sandy sites. This could indicate that soil water redistribution as influenced by topography in these sites with >80% sand (Table 1) was only minimal if not absent. Because the WFPS (which controls the aeration status of the soil) did not differ, this also might have resulted to the comparable N_2O fluxes between the landform complexes from the sandy sites. The N_2O emissions from these sandy sites differed between landform complexes (higher on the footslopes than on the shoulders) only during the spring, when the snow redistribution by wind had resulted in higher snow accumulation and wetter conditions on the footslopes than on the shoulders. The correlation coefficients between the measured and predicted WFPS from this sandy, fertilized oat site were 0.72 ($P = 0.01$) on the shoulder and 0.79 ($P = 0.001$) on the footslope.

For the fertilized cropped sites in the clay loam and fine sandy loam area, the N_2O fluxes differed between landform complexes (lower fluxes on the shoulder than on the footslope complex). However, the N_2O fluxes from both textural sites did not differ when compared at the landform complex level. Similar results were also observed for the measured WFPS. The correlation coefficients between the measured and predicted WFPS were ranging from 0.37 ($P = 0.07$) on the shoulder complex of the fine sandy loam site to 0.72 ($P = 0.001$) on the shoulder complex of the clay loam site.

Annual estimates of N_2O emissions

The estimates of annual N_2O emissions from the pasture sites (Table 4) were about half of the estimates from other studies: 0.100 kg N_2O-N ha^{-1} yr^{-1} for Wisconsin prairie (Goodroad & Keeney 1984), and 0.142 kg N_2O-N ha^{-1} yr^{-1} for Colorado shortgrass steppe (averaged from fertilized and unfertilized pastures; Mosier et al. 1996). The estimates of annual N_2O emissions from the forest sites were within the range of the estimates from pine and hardwood forest in the northeastern U.S., which were 0.010 ± 0.015 and 0.017 ± 0.017 kg N_2O-N ha^{-1} yr^{-1}, respectively (Bowden et al. 1990). On the other hand, Elliott & de Jong (1992) reported total denitrification losses (measured by C_2H_2 incubation method) of 1.0–1.4 kg N ha^{-1} on the shoulders and 7.6–12.8 kg N ha^{-1} on the footslopes from fertilized cropped sites in loam-textured Black soil zone (Udic Boroll) of Saskatchewan, Canada. In the present study, the estimates of N_2O emissions on the shoulders at the clay loam and fine sandy loam, fertilized cropped sites were comparable to their estimates of total denitrification losses. However, the estimates of N_2O emissions on the footslopes were about an order of magnitude lower than their estimates of total denitrification losses. These findings imply that on the footslopes, where reduced-O_2 conditions are common, N_2O emissions could be lower than total denitrification losses because of further reduction of N_2O to N_2.

In Ontario, Canada, Burton & Beauchamp (1994) examined the profile of N_2O concentrations in a soil subject to freezing. They observed accumulations of N_2O during the winter in the soil beneath the frozen layer. The pulse of activity in spring was attributed, in part, to the thawing of the frozen layer that permit release of N_2O trapped below it. In the present study, we measured N_2O emissions intensively during the spring (i.e., mid-March to April). A pulse of N_2O emission activity was detected during the spring thaw, and was related to the pattern of the melting of snow and thawing of the soil (i.e., low N_2O fluxes at the start of spring thaw, increased towards the mid-spring when the soil has the highest moisture content, and decreased towards the end of spring when the surface soil was already dry; (Corre et al. 1996)). In the clay loam and fine sandy loam, fertilized cropped sites, the spring emissions

Table 4. Seasonal and annual N_2O fluxes, areal extent, and extrapolated N_2O fluxes for the transitional grassland-forest region in the Black soil zone of Saskatchewan, Canada.

Land use–soil texture	Landscape scale						Regional scale	
	Landform complex	Proportion of area (%)	May to Oct	Spring	Annual	Weighted[1] annual flux	Area[2] (km^2)	Total annual flux (Mg N_2O-N yr^{-1})
			kg N_2O-N ha^{-1} yr^{-1})					
Fertilized cropped								
Sandy	Shoulder	40	0.032	0.042	0.074	0.162	285	4.62
(sandy, oat)[3]	Footslope	60	0.033	0.187	0.220			
Medium	Shoulder	50	1.137	0.112	1.249	2.368	991	235.67
(fine sandy loam, canola)	Footslope	50	2.710	0.823	3.533			
Moderately fine–fine	Shoulder	55	1.513	0.167	1.680	2.279	613	139.70
(clay loam, wheat)	Footslope	45	2.789	0.223	3.012			
Pasture								
Sandy	Shoulder	30	0.001	0.001	0.002	0.041	236	0.97
(sandy, alfalfa)	Footslope	70	0.004	0.053	0.057			
Medium–fine	1993–94		0.023	0.013	0.036	0.042	544	2.28
(clay loam, bromegrass; shoulder complex)	1994–95		0.023	0.024	0.047			
Forest								
Sandy	Shoulder	45	0.001	0.001	0.002	0.003	796	0.24
(sandy, aspen)	Footslope	55	0.001	0.003	0.004			
Medium–fine	1993–94		0.019	0.023	0.042	0.033	555	1.83
(clay loam, aspen; footslope complex)	1994–95		0.020	0.004	0.024			
Total							**4020**	**385**

1 The total annual N_2O fluxes were weighted by the areal coverage of the landform complexes at each study site.
2 Total area was determined from the combined land use and soil texture GIS layer (Figures 1 & 2).
3 The study sites representing the soil texture and land use characteristics in the study region.

accounted for an average of 9% and 15% of the annual N_2O fluxes on the shoulders and footslopes, respectively. In the sandy, fertilized oat site, the spring emissions contributed 57% and 85% of the annual N_2O fluxes on the shoulders and footslopes, respectively. In the uncultivated sites (pasture and forest sites), the averaged contributions of spring emissions to annual N_2O fluxes were 47% on the shoulders and 60% on the footslopes. Therefore, where labor limitation is an issue in obtaining representative measurements for annual estimate of N_2O emission, sampling effort in low-flux soils (e.g., forest, pasture, and sandy soils) could be focused during the spring period when most of the N_2O is evolved, while N_2O sampling in high-flux soils (e.g., fertilized, fine-textured soils) should be intensive during the growing season and the spring period when the effect of soil moisture combined with fertilization occurred.

The fertilizer-induced N_2O emission (% N_2O-N = {[annual N_2O flux from fertilized cropland – annual N_2O flux from unfertilized cropland]/fertilizer rate}) was calculated from the clay loam site, where emissions during both unfertilized (1993 growing season) and fertilized (1994 growing season) conditions were determined. Considering that 1993 and 1994 had weather conditions characterizing that of a normal year, it is reasonable to assume that the background annual N_2O flux during the unfertilized condition in 1993 (0.08 and 0.20 kg N_2O-N ha^{-1} yr^{-1} on the shoulder and footslope complexes, respectively) would be similar for 1994. The fertilizer rate applied to this site (a total of 85 kg N ha^{-1}) is a typical level that farmers use for this type of soil in the study region. The estimates of annual N_2O fluxes during the fertilized condition in 1994 comprised 2% and 3% of the applied N on the shoulder and footslope complexes, respectively.

Regional estimates of N_2O emissions

The average annual fluxes for fertilized cropped, pasture/hay land, and forest areas in this region, weighted by their areal extents in the different textural areas, were 2.00, 0.04, and 0.02 kg N_2O-N ha^{-1} yr^{-1}, respectively. The weighted-average annual fluxes for the medium- to fine-textured and sandy-textured areas were 1.40 and 0.04 kg N_2O-N ha^{-1} yr^{-1}, respectively. The weighted-average flux for the study region is 0.95 kg N_2O-N ha^{-1} yr^{-1}. Considering all the textural areas, the pasture/hay land and forest covered 53% of the total area in the study region and contributed less than 2% of the total regional flux. The fertilized cropped areas covered only 47% of the regional area, but contributed more than 98% of the regional flux.

The relationships between annual N_2O fluxes and soil texture (as exemplified by% sand), soil total N, and soil total organic C (Table 1) were examined for the fertilized cropped landscapes (Figure 4). The percentage sand was used as an index of the gradient of soil moisture regimes in the study region. The soil total N and organic C are the long-term integrative products of physical and biological factors, and were used as indices of the gradient of soil fertility in the study region. The present study showed that soil texture, total N and organic C explained most of the variations of annual N_2O emissions from fertilized cropped landscapes in this study region. Similar results were obtained by Groffman & Tiedje (1989), who showed that soil texture and drainage accounted for 86% of the variation of annual denitrification losses in temperate forest landscapes. These findings also imply that placing the investigation scheme in the context of the regional-scale factors that control N_2O emission would aid in overcoming the variability problem of quantifying N_2O emission at regional scales.

The calculation of regional-scale estimates based on site-specific data is always, however, dependent on a large number of assumptions. The sensitivity of the final estimates produced to these assumptions is difficult to assess, but both the landscape-specific emission estimates based on the WFPS-climate relationships and the soil survey/land use database used in regional extrapolation are subject to error. The development of a rigorous error estimate for the regional estimates is beyond the scope of this paper – indeed the degree of accuracy in the standard soil survey reports used to develop the textural classes remains a contentious point overall in these 'measure and multiply' exercises. Clearly the regional estimate produced would be very susceptible to, for example, variations in the rate of fertilizer inputs in the cultivated area of the region; nonetheless we believe the estimates produced provide a reliable measure of the N_2O emission under the stated assumptions used in our analysis.

In conclusion, our results showed that N fertilization in agricultural systems is the main source of soil-emitted N_2O from this study region. Even in this semiarid to subhumid cold continental region, the fertilizer-induced N_2O emission (2–3% from the clay loam, cropped site) was higher than the 1.25% yr^{-1} recommended globally (Bouwman 1994). We found that WFPS was the soil variable most correlated to N_2O emissions. This prompted us to use the method of estimating total N_2O emissions by using simple regression equations that relates WFPS to N_2O emission. There is, however, no possibility to link this to national inventory calculations. The OECD/IPCC (1991) program on national inventories of N_2O emission has based the calculation on the fertilizer rate, fertilizer type, and crop type. This calculation method, however, is greatly limited by the insufficiency of data available at present for calculating fertilizer type and crop type emission coefficients. We suggest a simple way of estimating fertilizer-induced N_2O emissions from agriculture by stratification according to soil moisture regime and fertilizer application

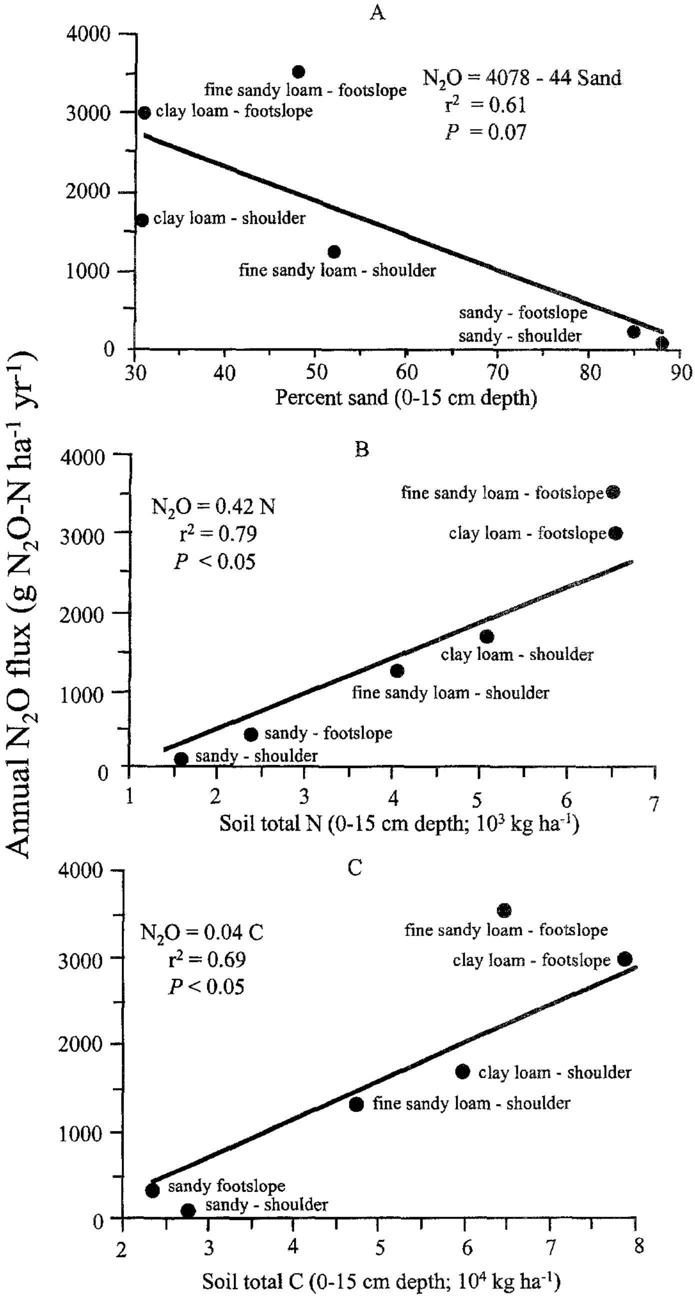

Figure 4. Relationships between annual N_2O fluxes and percent sand (a), total N (b), and total organic C (c) from fertilized cropped landscapes.

rates. In Canada, or Saskatchewan in particular, where farmers within a specific soil and climatic region would apply known amounts of fertilizers over the years and the soil moisture regime can readily be deduced from soil maps and GIS soil data base, N_2O emissions could be well represented.

Acknowledgements

This study was funded by Agriculture and Agri-Food Canada Greenhouse Gas and Climate Change Initiatives. The technical assistance of R. Anderson and C. Wong and the cooperation of the farmers and the Conservation Learning Center, especially P. Flaten, are highly recognized. The valuable suggestions of the reviewers are also greatly appreciated.

References

Acton DF & Ellis JG (1978) The Soils of the Saskatoon Map Area 73-B. Saskatchewan Institute of Pedology Pub. S4. Saskatchewan, Canada

Baier W & Robertson GW (1965) Estimation of latent evaporation from simple weather observations. Can. J. Plant Sci. 45: 276–284

Bouwman AF (1994) Direct Emission of Nitrous Oxide from Agricultural Soils. National Institute of Public Health and Environmental Protection. Report No. 773004004. Bilthoven, Netherlands

Bowden RD, Steudler PA, Melillo JM & Aber JD (1990) Annual nitrous oxide fluxes from temperate forest soils in the Northeastern United States. J. Geophys. Res. 95: 13997–14005

Burton DL & Beauchamp EG (1994) Profile nitrous oxide and carbon dioxide concentrations in a soil subject to freezing. Soil Sci. Soc. Am. J. 58: 115–122

Corre MD (1997) Landscape- and Regional-Scale Quantification of Nitrous Oxide Emission from a Subhumid Transitional Grassland-Forest Region. Ph. D. thesis, University of Saskatchewan, Saskatoon, Saskatchewan, Canada. 171 pp

Corre MD, van Kessel C & Pennock DJ (1996) Landscape and seasonal patterns of nitrous oxide emissions in a semiarid region. Soil Sci. Soc. Am J. 60: 1806–1816

Crutzen PJ & Ehhalt DH (1977) Effects of nitrogen fertilizers and combustion in the stratospheric ozone layer. Ambio 6: 112–117

Davidson EA & Hackler JL (1994) Soil heterogeneity can mask the effects of ammonium availability on nitrification. Soil Biol. Biochem. 26: 1449–1453

Elliott JA & de Jong E (1992) Quantifying denitrification on a field scale in hummocky terrain. Can. J. Soil Sci. 72: 21–29

Goodroad LL & Keeney DR (1984) Nitrous oxide emission from forest, marsh, and prairie ecosystems. J. Environ. Qual. 13: 448–452

Groffman PM (1991) Ecology of nitrification and denitrification in soil evaluated at scales relevant to atmospheric chemistry. In: Rogers JE & Whitman WB (Eds) Microbial Production and Consumption of Greenhouse Gases: Methane, Nitrogen Oxides, and Halomethanes (pp 201–217). Am. Soc. Microbiol., Washington, DC

Groffman PM & Tiedje JM (1989) Denitrification in north temperate forest soils: Relationship between denitrification and environmental factors at the landscape scale. Soil Biol. Biochem. 21: 621–626

Khalil MAK & Rasmussen RA (1992) The global sources of nitrous oxide. J. Geophys. Res. 97: 14651–14660

Krogman KK & Hobbs EH (1976) Scheduling Irrigation to Meet Crop Demands. Agriculture Canada, Ottawa, Ontario, Canada. Publ. 1590. 18 pp

Li C, Frolking SE & Frolking TA (1992) A model for nitrous oxide evolution from soil driven by rainfall events: I. Model structure and sensitivity. J. Geophys. Res. 97: 9759–9776

Matson PA & Vitousek PM (1990) Ecosystem approach to a global nitrous oxide budget. BioScience 40: 667–672

Matson PA, Vitousek PM & Schimel DS (1989) Regional extrapolation of trace gas flux based on soils and ecosystems. In: Andreae MO & Schimel DS (Eds) Exchange of Trace Gases Between Terrestrial Ecosystems and the Atmosphere (pp 97–108). Dahlem Workshop Report, John Wiley and Sons, Chichester, England

Mosier AR, Parton WJ, Valentine DW, Ojima DS, Schimel DS & Delgado JA (1996) CH_4 and N_2O fluxes in the Colorado shortgrass steppe: 1. Impact of landscape and nitrogen addition. Global Biogeochem. Cycles 10: 387–399

Myrold DD (1988) Denitrification in ryegrass and winter wheat cropping systems of western Oregon. Soil Sci. Soc. Am. J. 52: 412–416

OECD/OCDE (1991) Estimation of greenhouse gas emissions and sinks. Final report from the OECD experts meeting, 18–21 February 1991. Prepared for Intergovernmental Panel on Climate Change. Revised August 1991

Parsons LL, Murray RE & Smith MS (1991) Soil denitrification dynamics: Spatial and temporal variations of enzyme activity, populations, and nitrogen gas loss. Soil Sci. Soc. Am. J. 55: 90–95

Parton WJ, Mosier AR, Ojima DS, Valentine DW, Schimel DS, Weier K & Kulmala AE (1996) Generalized model for N_2 and N_2O production from nitrification and denitrification. Global Biogeochem. Cycles 10: 401–412

Pennock DJ, van Kessel C, Farrell RE & Sutherland RA (1992) Landscape-scale variations in denitrification. Soil Sci. Soc. Am. J. 56: 770–776

Pennock DJ, Zebarth BJ & de Jong E (1987) Landform classification and soil distribution in hummocky terrain, Saskatchewan, Canada. Geoderma 40: 297–315

Potter CS, Matson PA, Vitousek PM & Davidson EA (1996) Process modeling of controls on nitrogen trace gas emissions from soils worldwide. J. Geophys. Res. 101: 1361–1377

Robertson GP (1993) Fluxes of nitrous oxide and other nitrogen trace gases from intensively managed landscapes: A global perspective. In: Harper LA, Mosier AR, Duxbury JM & Rolston DE (Eds) Agricultural Ecosystem Effects on Trace Gases and Global Climate Change (pp 95–108). ASA Spec. Publ. 55. ASA, CSSA, and SSSA, Madison, Wisconsin

Rodhe H (1990) A comparison of the contribution of various gases to the greenhouse effect. Science 248: 1217–1219

Schimel DS & Potter CS (1995) Process modelling and spatial extrapolation. In: Matson PA & Harriss RC (Eds) Biogenic Trace Gases: Measuring Emissions from Soil and Water (Methods in Ecology Series) (pp 358–383). Blackwell Sci. Publ., Cambridge, Massachusetts

Schimel DS, Simkins S, Rosswall T, Mosier AR & Parton WJ (1988) Scale and the measurement of nitrogen gas fluxes from terrestrial ecosystems. In: Rosswall T, Woodmansee RG & Risser PG (Eds) Scales and Global Change (pp 179–193). SCOPE 35, John Wiley, New York

Schimel JP, Jackson LE & Firestone MK (1989) Spatial and temporal effects on plant-microbial competition for inorganic nitrogen in a California annual grassland. Soil Biol. Biochem. 21: 1059–1066

Schwab GO, Fangmeier DD, Elliott WJ & Frevert RK (1993) Soil and Water Conservation Engineering. 4th edn. John Wiley and Sons Inc., New York. 507 pp

Watson RT, Rodhe H, Oeschger H & Siegenthaler U (1990) Greenhouse gases and aerosols. In: Houghton JT, Jenkins GJ & Ephramus JJ (Eds) Climate Change: The IPCC Scientific Assessment (pp 7–40). Cambridge University Press, Cambridge, England

Weier KL, Doran JW, Power JF & Walters DT (1993) Denitrification and the dinitrogen/nitrous oxide ratio as affected by soil water, available carbon, and nitrate. Soil Sci. Soc. Am. J. 57: 66–72